Comparison of Industrial Tomography Algorithms for Gamma Scanning 2-D Reconstruction

Hae Yong Kim[1], M. I. Haraguchi[2], W.A.P. Calvo[3]

1 - Universidade de São Paulo, Escola Politécnica
Av. Prof. Luciano Gualberto, tr. 3, 158 - São Paulo - Brazil
hae@lps.usp.br

2 - Tricom Tecnologia
Av. Conselheiro Rodrigues Alves, 58 - Piquete - Brazil
marcio@tricomtecnologia.com.br

3 - Nuclear and Energy Research Institute – IPEN/CNEN-SP
Av. Prof. Lineu Prestes, 2242 - São Paulo - Brazil
wapcalvo@ipen.br

ABSTRACT

In this paper, we compare different industrial tomography algorithms to present the result of gamma scanning as a two-dimensional image of density distribution. In two-dimensional gamma scanning, an unconventional irradiation geometry is used and consequently many classic image reconstruction algorithms cannot be used. We tested two iterative reconstruction methods: ART (Algebraic Reconstruction Technique) and MART (Multiplicative Algebraic Reconstruction Technique). The iteration steps of both methods were intercalated with various filters: mean filter, median filter, anisotropic diffusion and total variation. The use of these filters greatly improves the quality of reconstruction. We report the obtained results.

Keywords Tomography Algorithm, Algebraic Reconstruction Technique, Multiplicative Algebraic Reconstruction Technique, Gamma Scanning, Industrial Tomography.

1 Introduction

Gamma ray column profiling or simply gamma scanning is a technique widely used to evaluate the mechanical and operational behavior of equipments. In this technique, a radioactive source and detector are positioned in opposite sides of the equipment and move along its length. The measured radiation attenuation values result in the profile of longitudinal density (figure 1).

In another paper we present in this conference (Haraguchi 2016), we introduce “Improved Gamma Scanning”, where the result of the gamma scanning is presented as a 2-D image of densities instead of 1-D graph. In order to generate 2-D image from gamma ray irradiation data, it is necessary to use industrial tomography algorithms. However, peculiar irradiation geometry used in the gamma scanning (figure 2) hinders the use of many classic image reconstruction algorithms. Usually, parallel geometry or fan-beam geometry is used in industrial tomography to reconstrct the density inside a circular section. Gamma ray profiling has a very different geometry and we want to reconstruct the density inside a rectangle section (instead of a circular section).

This paper describes the reconstruction techniques we used to reconstruct gamma scanning. We tested two iterative reconstruction methods: ART (Algebraic Reconstruction Technique) and MART (Multiplicative Algebraic Reconstruction Technique). The iteration steps of both methods were intercalated with various filters: mean filter, median filter, anisotropic diffusion and total variation. The use of these filters greatly improves the quality of reconstruction. We report the obtained results.

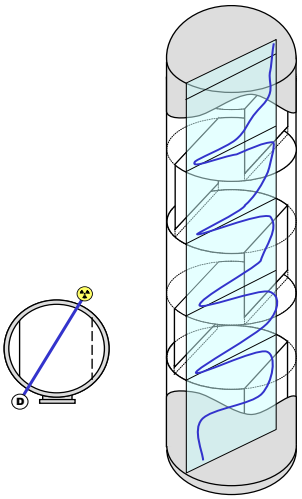

Figure 1: In gamma scanning, a radioactive source and detector are positioned in opposite sides of the equipment and move along its length (extracted from Haraguchi 2013).

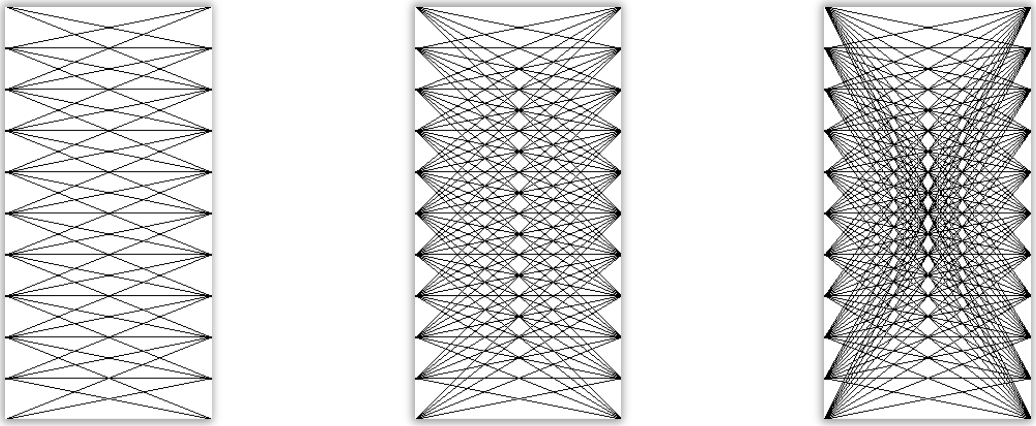

(a) Aperture ±40cm. (b) Aperture ±100cm. (c) Aperture ±200cm.

Figure 2: The peculiar geometry used in gamma scanning hinders the use of many classic reconstruction algorithms. The rectangle to be reconstructed has dimension 200cm x 100cm and the spacing between two consecutive positions is 20cm.

2 Theory

2.1 Computer tomography and ART/MART reconstruction algorithms

Let $\mu(x, y)$ be the spatial distribution of the coefficient of attenuation of gamma ray; I_o the emitted radiation intensity; and I_d the detected radiation intensity. Then, the following proportionality holds:

$$\frac{I_d}{I_o} \propto \left[\frac{d}{d_o}\right]^2 \exp\left[-\int \mu(x,y)dr\right]$$

where r is the path followed by the gamma ray; d/d_o is the relative distance between the ray emissor and detector in relation to a "standard distance" d_o. Rewriting the equation:

$$b = -\ln\left(\frac{I_d}{I_o}\left[\frac{d}{d_o}\right]^2\right) \propto \int \mu(x,y)dr$$

Let us call "measured projection" b the left term of the proportionality. The tomographic reconstruction problem is to determine the spatial distribution of attenuation $\mu(x, y)$ given many measured projections b in many geometrically different ray paths r.

The Algebraic Reconstruction Technique (ART) is an iterative algorithm used in computed tomography. It reconstructs an image from a series of projections. Gordon et al. (1970) first showed its use in image reconstruction.

ART can be considered as an iterative solver of a system of linear equations ***Ax=b***. The values of reconstructed image pixels are the variables of the vector ***x*** (the attenuation coefficients $\mu(x, y)$), each row a_i of the matrix ***A*** is the path of the *i*-th gamma ray (the geometry of ray *r*) and the measured projections form the vector ***b***. The formula below computes an approximation of the solution of the linear systems of equations:

$$x^{k+1} = x^k + \lambda_k \frac{b_i - \langle a_i, x^k \rangle}{\|a_i\|^2} (a_i)^t$$

where $i = (k \bmod m) + 1$ and λ_k is a relaxation parameter. In simple case, the matrix ***A*** consists of only 1's and 0's:

$$a_{ij} = \begin{cases} 1, \text{ if ray } i \text{ passes through pixel } j. \\ 0, \text{ otherwise.} \end{cases}$$

and $\|a_i\|^2$ becomes the number of pixels that the ray *i* passes through (number of 1's in a_i). In this simple case, MART can be written as:

$$x^{k+1} = x^k \otimes \left[\left(\frac{b_i}{\langle a_i, x^k \rangle} \right)^{\lambda_k} (a_i)^t \right]$$

where $\otimes$ indicates Hadamard product (elementwise product). While ART converges in the consistent case to a minimal norm solution, MART is designed to converge to a solution that minimizes the entropy (Natterer 1998).

Replacing $i = (k \bmod m) + 1$ by a randomly chosen indice, we obtain randomized ART and randomized MART that we actually use in our experiments. Moreover, in our implementation, the relaxation parameter λ_k decreases as the iteration step *k* increases. We noted experimentally that this improves the quality of the reconstruction.

2.2 Distortion measures

In order to compare different tomography algorithms with different parameters, it is necessary to measure how different are two images (spatial distribution of attenuation coefficients). We consider three kinds of measures:

2.2.1. Mean of pixelwise differences (MAE, RMSE, PSNR).

Mean absolute error (MAE), root of mean square error (RMSE) and peak signal to noise ratio (PSNR). The three measures are closely related and measures pixelwise difference between the two images. Given an ideal image *F* and an estimated image $\hat{F}$ both with *J*x*K* pixels, their definition are:

$$MAE = \frac{\sum_j \sum_k \left| F(j,k) - \hat{F}(j,k) \right|}{J \times K}$$

$$RMSE = \sqrt{\frac{\sum_j \sum_k \left(F(j,k) - \hat{F}(j,k) \right)^2}{J \times K}}$$

$$PSNR = 20 \log_{10} \left(\frac{\max\{F(j,k)\}}{RMSE} \right)$$

This kind of measure seems to be the most used for comparing the quality of tomography algorithms. However, this measure cannot be used if the reconstruction algorithm does not preserve the mean density, like some filtered backprojections. It also will not measure fairly the distortion if the

reconstruction algorithm does not evaluate correctly the absolute density, even though it succeeds in reconstructing the density changes.

2.2.2. Modular transfer function (MTF).

This function is usually used to describe the lens performance and it measures the transfer of modulation (or contrast). A series of high contrast bars is presented to the imaging system (figure 3). The imaging system will blur the bars. MTF in a fixed resolution is computed as:

MTF = (maximum intensity - minimum intensity)/(maximum intensity + minimum intensity)

Computing MTF in many resolutions, we obtain the graph MTF versus lp/mm (line pairs per milimeter).

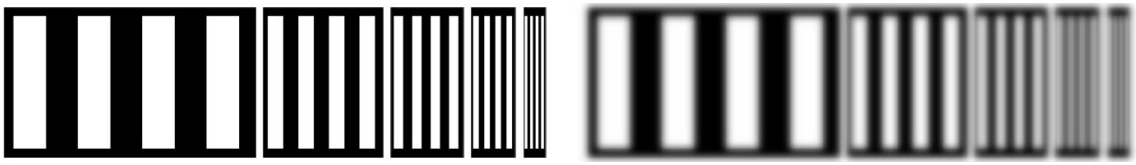

Figure 3: A series of bars in different resolutions is used to compute MTF (modular transfer function).

This is a good measure for imaging systems that blurs the image. However, it cannot be used if the imaging system produces (for example) aliased images. In figure 4, the original phantom at left has 13 high density regions (white bars). The reconstructed image at right has high contrast and consequently high MTF. However, it presents only 7 high density regions. So, this reconstruction would be measured as presenting high quality using MTF.

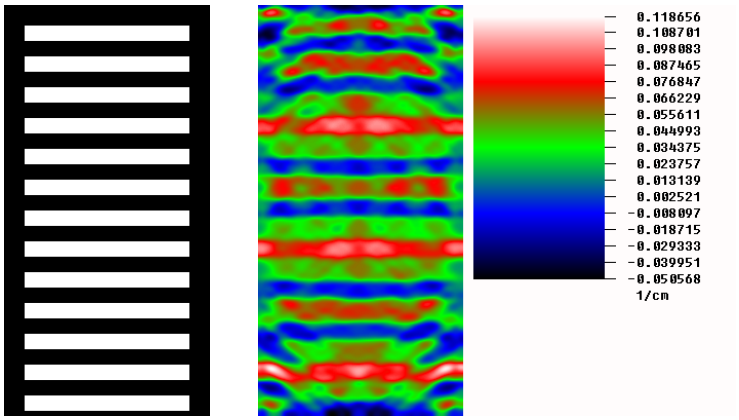

Figure 4: (Left) the original density distribution with 13 high density regions (black=attenuation zero and white=attenuation 0.1). (Right) the reconstructed aliased image with 7 high density regions.

2.2.3. Strutural similarity (SSIM)

To compute the similarity of two images *X* and *Y*, strutural similarity (Wang 2004) uses sliding window and computes the similarity of the contents *x* and *y* of the two windows. The structural similarity of the images X and Y is the average similarity of the windows in all positions of the images. Let *x* and *y* be two vectors obtained by copying the contents of the windows of images *X* and *Y*. The similarity of luminosity is:

$$l(x,y) = \frac{2\mu_x\mu_y + C_1}{\mu_x^2 + \mu_y^2 + C_1}$$

where μ_x is the mean value of vector *x*; C_1 is a small number to avoid numerical instability when the means are close to zero. This function returns a number between 0 and 1. The similarity of contrast is:

$$c(x,y) = \frac{2\sigma_x\sigma_y + C_2}{\sigma_x^2 + \sigma_y^2 + C_2}$$

where σ_x is the standard deviation of vector *x*; C_2 is another small number. This function also returns a number between 0 and 1. The similarity of structure is:

$$s(x,y) = \frac{\sigma_{xy} + C_3}{\sigma_x \sigma_y + C_3}$$

This function computes the correlation coefficient between the vectors *x* and *y* and returns a number between -1 and +1. The final similarity measure is computed as:

$$SSIM(x,y) = [l(x,y)]^{\alpha} [c(x,y)]^{\beta} [s(x,y)]^{\gamma}$$

where α, β and γ are the weights of brightness, contrast and structure. Usually, $\alpha = \beta = \gamma = 1$.

3 Experiments

To simulate the gamma scanning, we constructed different phantoms. All them are rectangles with dimensions 200cm x 100cm and are represented by images with 400 x 200 pixels. All phantoms have only two different attenuation coefficients: 0/cm represented by black and 0.1/cm represented by white. To standardize the tests, we always use consecutive gamma sources/detectors spaced 20 cm with maximum aperture of ±200cm (figure 2c).

3.1 Horizontal bars

We generated the phantom shown in figure 5a with 5 horizontal bars with height 20 cm (40 pixels) and run the algorithms ART and MART without any filter, obtaining the reconstructions 5b and 5c. We used the simulated ray width of 31 pixels, 10 iterations with relaxation parameter λ decreasing linearly from 1.0 to 0.1. The simulated rays are visible in the reconstructions. The mean absolute errors were respectively 23.5% and 28.2% of the maximum density (0.1/cm).

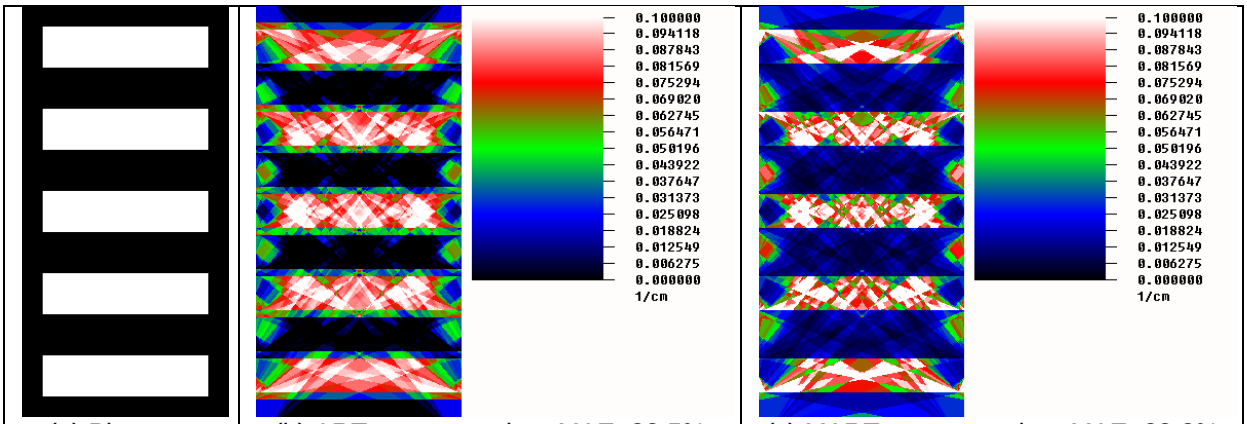

(a) Phantom (b) ART reconstruction. MAE=23.5% (c) MART reconstruction. MAE=28.2%

Figure 5: Reconstruction without any filtering.

The reconstruction can be improved intercalating appropriate filters between reconstruction steps (Bustos 2005). Figure 6 shows the results of the reconstruction intercalating mean and median filters (with windows 15 x 15 pixels) between the iterations steps of ART/MART reconstruction algorithms, obtaining visually much more pleasant reconstructions. The simulated rays are no more visible. As the reconstructions seems visually to be improved, we would expect that the measured error have decreased. Unfortunately, using mean filter (figures 6a and 6b), MAE actually increases. Using median filter (figures 6c and 6d), MAE remains unchanged using ART and decreases slightly using MART. However, the lowest MAE remains at 23.5% (ART without filter or ART with median filter). In all tests, ART has lower errors than MART. At this point, we can ask whether MAE is an appropriate metric for measuring the quality of the tomographic reconstruction.

As we already know that ART yields better reconstruction than MART, we will continue testing only ART. Intercalating robust anisotropic diffusion (Black1998) we obtain the reconstruction depicted in figure 7a. We iterated anisotropic diffusion 40 times using diffusion scale 0.1 between the iteration steps of ART, obtaining MAE 23.1%. Intercalating total variation minimization algorithm (Chambolle 2004; Peyré 2012), we obtained figure 7b with MAE 21.8%, the lowest error. The obtained reconstruction image has sharp edges.

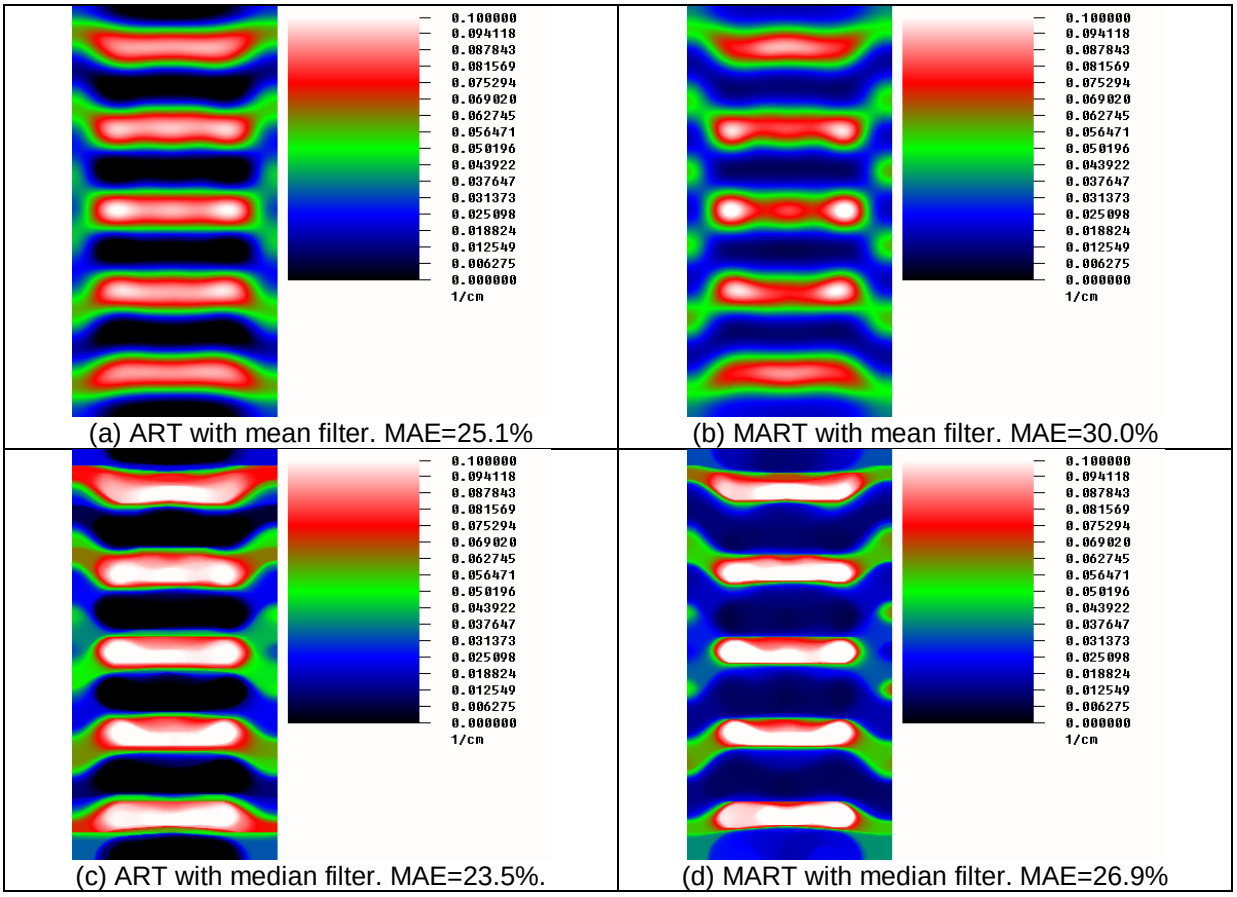

(a) ART with mean filter. MAE=25.1%

(b) MART with mean filter. MAE=30.0%

(c) ART with median filter. MAE=23.5%.

(d) MART with median filter. MAE=26.9%

Figure 6: Reconstruction with mean and median filters between iteration steps

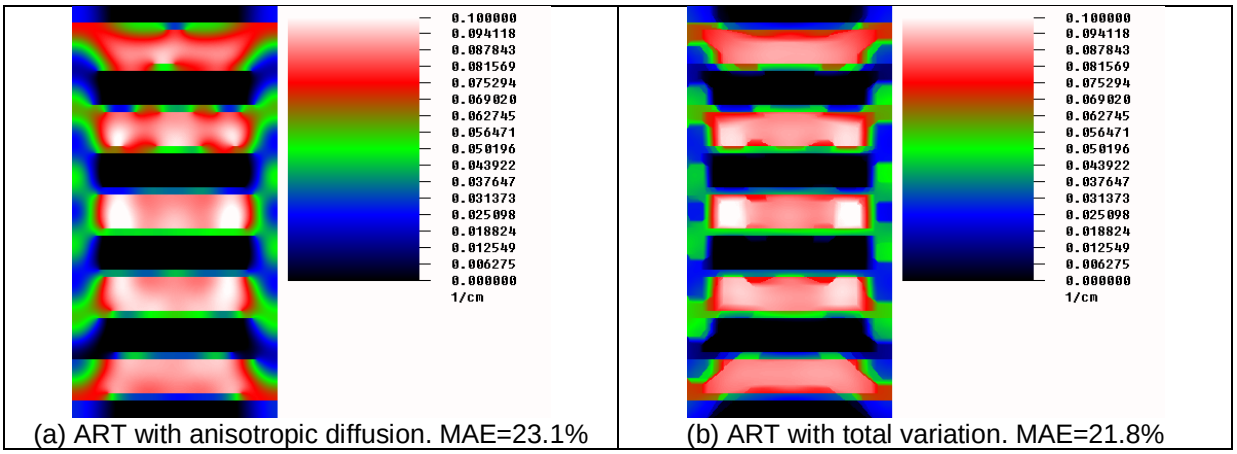

(a) ART with anisotropic diffusion. MAE=23.1%

(b) ART with total variation. MAE=21.8%

Figure 7: Reconstruction with anisotropic diffusion and total variation between iteration steps.

4 Conclusion

In this paper, we have compared many image reconstruction algorithms to present the result of gamma scanning as a two-dimensional image of density distribution. We tested ART and MART, intercalating different filters. The best result was obtained using ART with total variation minimization filter.

REFERENCES

Black, M. J.; Sapiro, G.; Marimont, D. H.; Hegger D. (Mar. 1998). “Robust Anisotropic Diffusion,” IEEE Trans. Image Processing, vol. 7, no. 3, pp. 421-432.

Bustos, H. I. A.; Kim, H. Y. (2005). “Reconstruction-Diffusion: An Improved Maximum Entropy Reconstruction Algorithm Based on the Robust Anisotropic Diffusion,” in Proc. Sibgrapi - Brazilian Symp. on Comp. Graph. and Image Proc..

Chambolle, A. (2004). “An algorithm for total variation minimization and applications,” Journal of Mathematical imaging and vision 20.1-2: 89-97.

Gordon, R; Bender, R; Herman, GT (1970). “Algebraic reconstruction techniques (ART) for three-dimensional electron microscopy and x-ray photography". Journal of Theoretical Biology 29 (3): 471–81.

Haraguchi, MI; Kim, HY; Calvo, WAP (2016). Distillation Column Troubleshooting with Improved Gamma Scan Technique. 8th World Congress on Industrial Process Tomography, Iguassu Falls, Brazil.

Haraguchi, MI (2013). Imageamento de Equipamentos Industriais pela Técnica de Perfilagem por Raios Gama. M.Sc. dissertation. Instituto de Pesquisas Energéticas e Nucleares, USP, Brazil.

Natterer F. (1998) “Numerical Methods in Tomography,” Universität Münster. Accessed on July 2016, http://wwwmath.uni-muenster.de/num/Preprints/1998/natterer_1/paper.html/fn.html

Peyré G. (2002). Total Variation Regularization with Chambolle Algorihtm, accessed on July 2016 http://www.coe.utah.edu/~cs7640/readings/Total%20Variation%20Regularization%20with%20Chambolle%20Algorihtm.pdf

Wang Z.; Bovik, A. C.; Sheikh, H. R.; Simoncelli, E. P. (April 2004). *Image Quality Assessment: From Error Visibility to Structural Similarity*, *IEEE T. Image Processing*, Vol. 13, No. 4, pp. 600-612.